A model differential equation for turbulence

Colm Connaughton
Laboratoire de Physique Statistique de l'Ecole Normale Supérieur, associé au CNRS, 24 Rue Lhomond, 75231 Paris Cedex 05, France

Sergey Nazarenko
Mathematics Institute, University of Warwick, Coventry CV4 7AL, United Kingdom
(Dated: April 20, 2003)

A phenomenological turbulence model in which the energy spectrum obeys a nonlinear diffusion equation is presented. This equation respects the scaling properties of the original Navier-Stokes equations and it has the Kolmogorov $-5/3$ cascade and the thermodynamic equilibrium spectra as exact steady state solutions. The general steady state in this model contains a nonlinear mixture of the constant-flux and thermodynamic components. Such "warm cascade" solutions describe the bottleneck phenomenon of spectrum stagnation near the dissipative scale. Self-similar solutions describing a finite-time formation of steady cascades are analysed and found to exhibit nontrivial scaling behaviour.

PACS numbers: 47.27.Eq, 47.27.Gs

I. MODEL EQUATION

In this article, we present a model equation for the energy spectrum of isotropic homogeneous turbulence,

$$E_t = \frac{1}{8}(k^{11/2}E^{1/2}(E/k^2)_k)_k + f - \nu k^2 E, \tag{1}$$

where t is time, k is the absolute value of the wavenumber, ν is the kinematic viscosity coefficient, f is an external forcing and the energy spectrum $E(k,t)$ is normalised so that the kinetic energy density is $\int E\, dk$. The third term on the RHS of this equation is obvious and describes the linear process of viscous dissipation. The first term contains a nontrivial model of the nonlinear processes in turbulence which rests on three basic properties[10]:

1. The total energy density $\int E\, dk$ is conserved by the inviscid dynamics. The characteristic time of the spectral energy redistribution for *local* interaction of turbulent scales is of order of the vortex turnover time, $1/\sqrt{k^3 E}$.

2. The steady state in forced turbulence corresponds to a constant energy cascade though the inertial range of scales which is described by the Kolmogorov spectrum,

$$E = C\, P^{2/3}\, k^{-5/3}, \tag{2}$$

where P is the energy flux (constant in t and k) and C is the Kolmogorov constant. Experimental measurements [1] give $C = 1.6 \pm 0.17$. As we will see below, equation (1) has an exact solution of form (2) with $C = (24/11)^{2/3} \approx 1.68$ (C can be changed by tuning the constant factor in the first term).

3. When the wave-number range is truncated to a finite value and both forcing and dissipation are absent, turbulence reaches a thermodynamic equilibrium state characterized by equipartition of energy over the wave-number space [2]. In terms of the one-dimensional energy spectrum this means $E \propto k^2$ which is obviously a steady state solution of the equation (1) for $f = \nu = 0$. Mathematical simplicity and respect to the above basic properties of Navier-Stokes turbulence make model (1) useful for practical and numerical applications. We will now analyze solutions of (1) in greater detail to find other properties that are predicted by this model.

II. STATIONARY SOLUTIONS

Let us consider steady-state spectra in the inertial range. For $f = \nu = 0$, we have the following general time-independent solution,

$$E = C\, k^2\, (P k^{-11/2} + Q)^{2/3}, \tag{3}$$

where $C = (24/11)^{2/3} \approx 1.68$ and P and Q are arbitrary constants. For $Q = 0$, this gives the pure Kolmogorov cascade solution (2), whereas for $P = 0$ this is a pure thermodynamic equilibrium. For the general solution, both the constant flux of energy $P = -\frac{1}{8}k^{11/2}E^{1/2}(E/k^2)_k \neq 0$ and a thermodynamic part ($Q \neq 0$) are present; they appear as an interesting nonlinear combination and not just as a linear superposition because equation (1) is nonlinear. Thus, one can refer to solution (3) with finite P and Q as a *warm cascade* to distinguish it from the pure Kolmogorov solution which could be viewed as a *cold cascade*.

Let us suppose that turbulence is produced near some scale $k = k_0$ so that $f(k) > 0$ only in a finite range in the vicinity of k_0. Suppose that $f(k) = 0$ to the left of this range (at large scales) and in a large inertial range to the right which ends at a very high $k \sim k_d$ where viscosity ν or some other dissipation mechanisms ($f(k) < 0$) become important. Then, up-scale of the forcing there will be a pure thermodynamic solution with $P = 0$ and $Q \neq 0$ because there is no dissipation or forcing assumed to be present near $k = 0$ to absorb or generate a finite energy flux. In the inertial range down-scale of the forcing there will be a constant flux cascade solution. This solution typically takes the form of a pure Kolmogorov (cold) cascade and extends down to the dissipation range where the energy flux is absorbed. Typically, the solution only penetrates a finite distance into the dissipation range and adapts itself until it provides sufficient dissipation to absorb the supplied flux. In the presence of dissipation, the model does not develop structure at arbitrarily high k as it would in the inviscid case. The qualitative features of the steady state are independent of the detailed form chosen for the dissipation. Figure 1 shows the steady state solutions obtained numerically for several different choices of the dissipation.

However, if the dissipation is not sufficiently strong, the solution can penetrate far enough into the dissipation range to reach the maximal wave-number which necessarily exists in any numerical solution. If one imposes a zero flux condition at the right end of the computational interval, the energy flux is reflected from the maximal wave-number leading to greater values of E in the dissipative range. Such a cascade stagnation acts to enhance the dissipation rate and thereby to adjust it to the energy flux to be absorbed. This phenomenon is common in numerical simulations of turbulence and is sometimes called the bottleneck phenomenon [3]. Figure 2 shows a numerically obtained steady state for the dissipation function,

$$\nu(k) = \begin{cases} \nu_0 (k - k_D)^2 & k \geq k_D \\ 0 & k < k_D \end{cases} \tag{4}$$

with $\nu_0 = 1.0 \times 10^{-5}$ and $k_D = 500$. The bottleneck phenomenon is clearly seen as an energy "pile up" over the cold cascade solution near the dissipative scale. In our model, the bottleneck phenomenon is described by the *warm* cascade solutions; in particular the theoretical curve in figure 2 is computed by taking $P \approx 14.5$, $Q \approx 1.5 \times 10^{-9}$ in equation (3). The relative importance of the "thermal" effects with respect to the cascade grows as one moves from larger to smaller scales; in extreme cases the spectrum can be nearly pure Kolmogorov near the forcing range and almost purely thermodynamic near the dissipative scale.

Because of the nonlinearity, solutions for given forms of forcing and dissipation are usually hard to find analytically and one has to use numerics. However, a lot of insight about the qualitative behavior of the system can be gained from considering stationary solutions (3) in an inertial range $k_1 < k < k_2$ and fixing the spectrum at its boundaries, $E(k_1) = E_1, E(k_2) = E_2$. This kind of the boundary conditions roughly models the forcing and the dissipation effects outside of the inertial range. This gives

$$P = [(E_2/Ck_2^2)^{3/2} - (E_1/Ck_1^2)^{3/2}]/(k_2^{-11/2} - k_1^{-11/2}) \tag{5}$$

$$Q = [k_2^{5/2}(E_2/C)^{3/2} - k_1^{5/2}(E_1/C)^{3/2}]/(k_2^{11/2} - k_1^{11/2}) \tag{6}$$

Thus, the sign of P is opposite to the sign of $(E_2/E_1 - k_2^2/k_1^2)$ and can be either positive or negative depending of the spectrum steepness with thermodynamic k^2 solution been a borderline case for which $P = 0$. Constant Q can also be either positive or negative with Kolmogorov $-5/3$ been the borderline slope. It is convenient to think of the $Q < 0$ solutions as negative temperature states.

III. NON-STATIONARY SOLUTIONS

So far we concentrated on the stationary solutions but how do these solutions form? We consider from now on the inviscid case. The Kolmogorov $-5/3$ spectrum is of a *finite capacity* type in that it contains only a finite amount of energy at the high k end. Let us take an initial condition which is compactly supported and force the system by imposing a constant flux boundary condition across the left end of the computational interval. Owing to the finite capacity of the Kolmogorov solution, an infinitely remote dissipative scale must be reached in a finite time. The solution has a nonlinear front at $k = k_*(t)$ and this front accelerates explosively, reaching $k = \infty$ at a finite singular time which we shall denote by t_*. We can equally consider the decaying case where an initial distribution of energy, compactly supported at large scales, is allowed to spread under the action of the nonlinearity without any external forcing. Provided there is sufficient energy in the initial condition, the right front still reaches $k = \infty$ within a finite

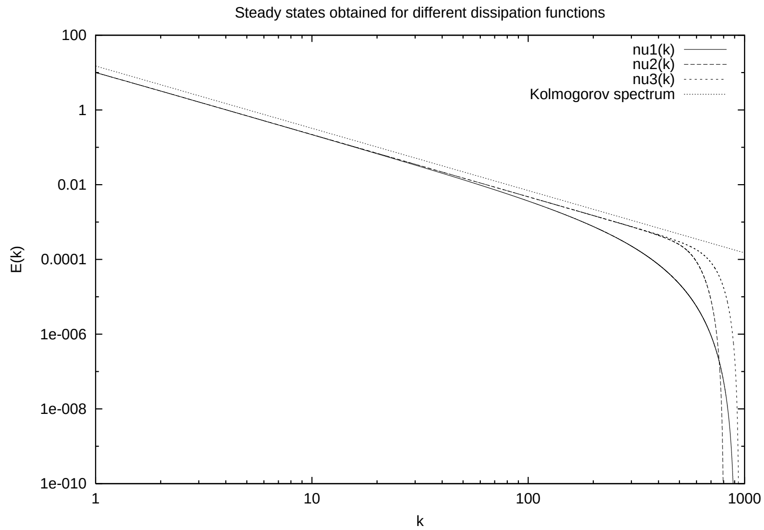

FIG. 1: Numerically computed steady states for several choices of dissipation function: $\nu_1(k) = (500-k)^2$, $\nu_2(k) = 4.0 \times 10^{-6}(500-k)^4$, $\nu_3(k) = 1.0 \times 10^{-2}k^2$. The Kolmogorov spectrum is also shown for comparison but shifted slightly for clarity.

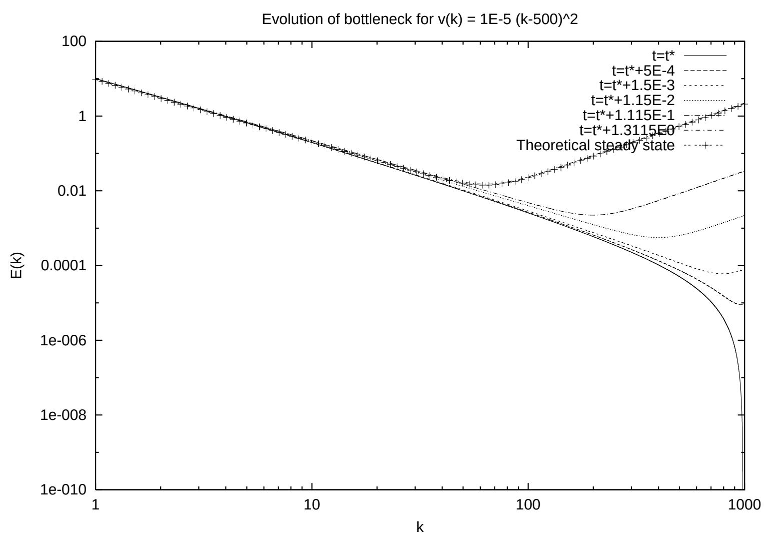

FIG. 2: Numerical evolution of a bottleneck for dissipation function $\nu(k) = 1.0 \times 10^{-5}(k-500)^2$. The resulting steady state is well described by the solution (3).

time but in addition a second front propagates to the left spreading the spectrum to large scales. This second front does not exhibit singular behaviour in finite time. Hence the decaying case is broadly similar to the forced case as far as large k behaviour is concerned since the initial concentration of energy at large scales acts as an effective forcing for the right front.

It is well known (see for example [4]) that the solutions of nonlinear diffusion equations with compactly supported initial data often have the property of remaining compactly supported during the time evolution. This turns out to be the case here. The left and right nonlinear fronts actually correspond to the left and right extrema of the support of the solution. Since these points must be determined as part of the solution, we are, in principle, required to solve a moving boundary problem with two free boundaries. In order that the problem be well-posed, we require an additional *moving boundary condition* on each interface[5]. For the problem under consideration, the appropriate

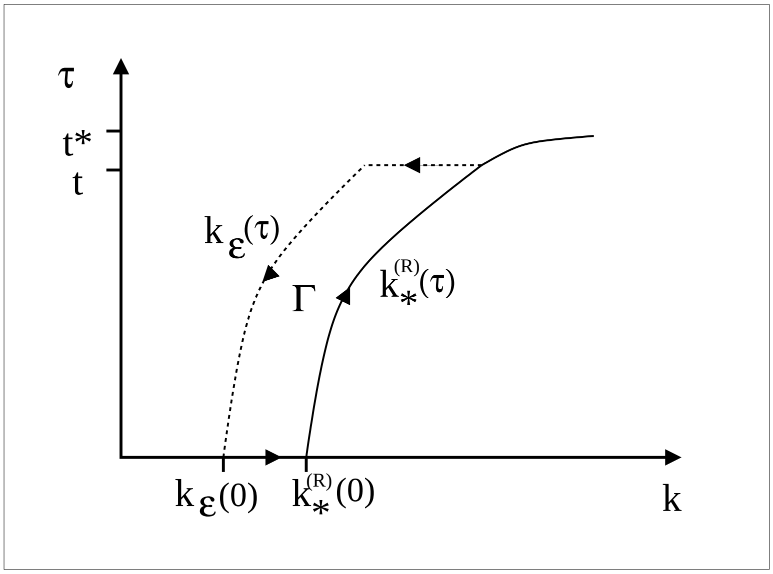

FIG. 3: Integration contour leading to the moving boundary condition, (7).

condition for the right front is

$$\frac{dk_*^{(R)}}{dt} = -\lim_{k\to k_*^{(R)}} k^{\frac{11}{2}} E^{-\frac{1}{2}} \frac{\partial}{\partial k}\left(k^{-2}E\right). \tag{7}$$

A similar condition holds for the left front.

Let us briefly explain how one arrives at this formula. It can be proven rigorously for the case of the porous medium equation as shown in [6]. Consider the time interval $[0,t]$ with $t < t^*$. For $0 < \tau < t$ the right interface is given by the curve $k_*^{(R)}(\tau)$ as shown in figure 3. Taking, $\epsilon << 1$ and assuming that the solution goes continuously to zero at the right interface we define the curve $k_\epsilon(\tau)$ by the condition $E(k_\epsilon(\tau),\tau) = \epsilon$ for $0 < \tau < t$. We now integrate over the region enclosed by the contour, Γ, in (k,t) plane as shown in the figure,

$$\int\!\!\int \left(\frac{\partial E}{\partial \tau} + \frac{\partial P}{\partial k}\right) dk\, d\tau = 0. \tag{8}$$

Applying Green's theorem, we reduce this to an integral over the contour, Γ,

$$\oint_\Gamma (E\, dk - P\, d\tau) = 0. \tag{9}$$

Proceed as follows

$$\oint_\Gamma E\left(dk - \tilde{P}\, d\tau\right) = 0, \tag{10}$$

where

$$\tilde{P} = -k^{\frac{11}{2}} E^{-\frac{1}{2}} \frac{\partial}{\partial k}\left(k^{-2}E\right). \tag{11}$$

Writing the contributions from the four sections of the curve Γ explicitly we have

$$\int_{k_*^{(R)}(\tau)} E\left(dk + \tilde{P}\, d\tau\right) + \int_{k_*^{(R)}(t)}^{k_\epsilon(t)} E\, dk + \int_{k_\epsilon(\tau)} E\left(dk + \tilde{P}\, d\tau\right) + \int_{k_\epsilon(0)}^{k_*^{(R)}(0)} E\, dk = 0. \tag{12}$$

Now, $E = 0$ on $k_*^{(R)}(\tau)$ and $E = \epsilon$ on $k_\epsilon(\tau)$. Using these facts we obtain

$$k_\epsilon(0) - k_\epsilon(t) - \int_t^0 \tilde{P}(k_\epsilon(\tau),\tau)\, d\tau = \int_{k_\epsilon(t)}^{k_*^{(R)}(t)} \frac{E}{\epsilon}\, dk - \int_{k_\epsilon(0)}^{k_*^{(R)}(0)} \frac{E}{\epsilon}\, dk. \tag{13}$$

We now take $\epsilon \to 0$ so that $k_\epsilon(\tau) \to k_*^{(R)}(\tau)$. The integrands on the RHS are bounded by 1 and therefore give no contribution. We are left with

$$k_*^{(R)}(t) = k_*^{(R)}(0) + \int_0^t \tilde{P}(k_*^{(R)}(\tau), \tau)\, d\tau, \tag{14}$$

which in conjunction with (11) yields (7) upon differentiation.

Let us now look for a self similar solution of equation (1) taking the following form

$$E = (t_* - t)^a F(\eta); \quad \eta = k/k_*, \quad k_* = c(t_* - t)^b, \tag{15}$$

where a, b and c are constants. Clearly, b must be negative since we require that $k_* \to \infty$ as $t \to t_*$. Substituting (15) into (1) with $f = \nu = 0$ we find that the t dependence drops out of the equation if $a = -2 - 3b$. We then have the following equation for F,

$$(3b+2)F + b\eta F' = \frac{C^{3/2}}{8}(\eta^{11/2} F^{1/2} (F/k^2)')', \tag{16}$$

where prime means differentiation with respect to η. Equation (16) defines a one-parameter family of self-similar solutions. Note that substitution of the form (15) into the moving boundary condition, (7) yields the same similarity relations. Thus the moving boundary condition is consistent with the similarity ansatz but does not provide any additional constraints. In particular it does not tell us which member of the 1 parameter family of solutions is selected by the PDE.

The solution near the front tip can be found by expanding F in series with respect to small $(1-\eta)$; in the leading order we have

$$F = \frac{16b^2}{C^3}(1-\eta)^2 \tag{17}$$

which gives for the spectrum

$$E = \frac{16b^2}{{k_*}^3 (t_* - t)^2}\left(1 - \frac{k}{k_*}\right)^2. \tag{18}$$

Notice that the quadratic decay of the solution as one approaches the tip is exactly the decay required in order to ensure that the speed of the tip as given by (7) is finite and non-zero.

We are interested in solutions which behave like a power law far behind the front. That is $E \sim k^{-x}$ as $k \to 0$. The relations (15) then imply that $x = -a/b$. The pure Kolmogorov spectrum, $x = 5/3$, therefore requires $b = -3/2$, corresponding to what one might consider to be normal scaling in the wake of the front.

We performed numerical simulations of the forced solutions of equation (1) with compact initial data and constant input flux on the left. We use the numerical solution to check the development of a self-similar front with tip of form (17) and to determine which value of b is selected. The results are shown in figure figure 4. The scaling parameter, b and the singular time, t_*, are most conveniently extracted from the relation

$$k_* \left(\frac{dk_*}{dt}\right)^{-1} = -\frac{1}{b}(t_* - t), \tag{19}$$

which allows one to calculate b and t_* from a linear fit of the data near $t = t_*$ as shown in figure 5. We find that $t_* = 0.0799$ and $b = -1.748$ which corresponds a significantly steeper than Kolmogorov slope, $x = 1.856$. The singular time, t_*, depends on the choice of initial conditions but the anomalous scaling exponent does not. In particular we verified that approximately the same value of b is obtained for the decaying case. The results for decaying turbulence are shown in figure 6. In figure 7 we fit the data to the relation (19) to obtain $t_* = 0.0154$ and $b = -1.739$. This gives $x = 1.850$. We expect that the small difference between the two cases will disappear if the simulations are extended closer to the singular time since the relation (19) is only expected to be true asymptotically.

Such anomalous scaling behavior whereby the exponent of the solution in the wake of the nonlinear front is larger than the Kolmogorov value has been observed before. Examples include MHD wave turbulence[7] and weak turbulence with local interactions[8]. We expect that this anomaly is a general property of finite capacity systems rather than a property of our model and therefore may also be present in the Navier-Stokes equations.

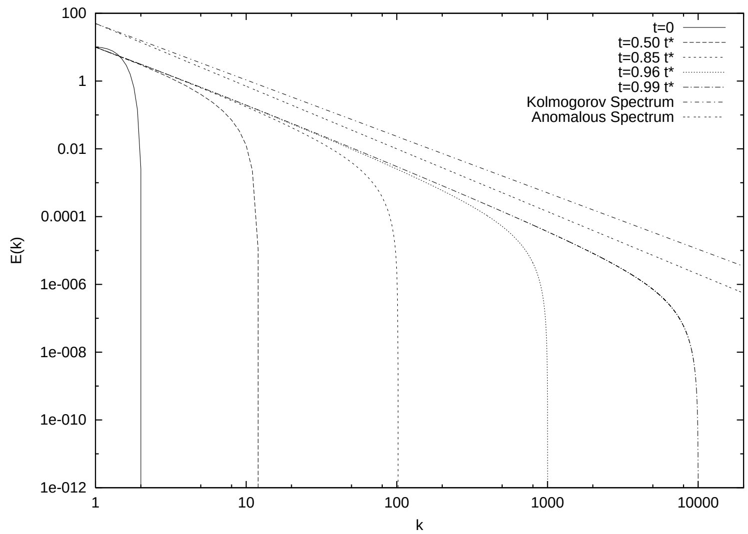

FIG. 4: Forced time-dependent solutions beginning from compact initial data showing development of self-similar front with power law wake.

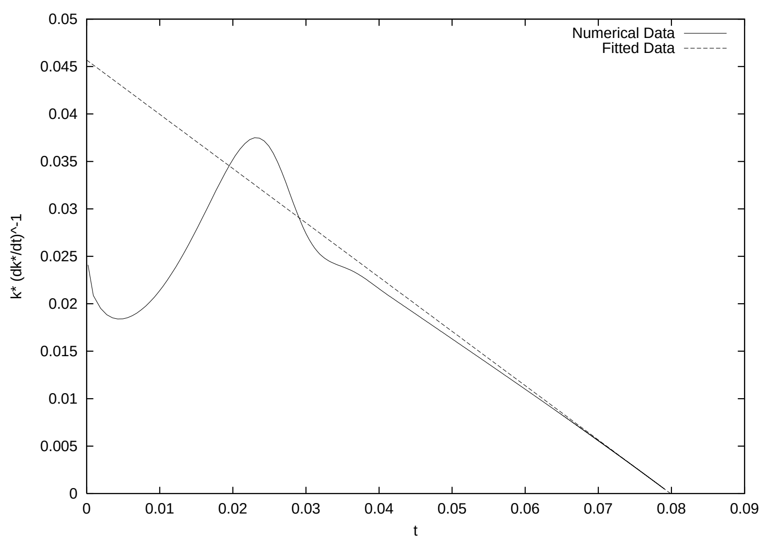

FIG. 5: Calculation of the asymptotic scaling properties of the self-similar solution for the forced case. The fitted line has $1/b = -0.572$ and $t^* = 0.0799$.

IV. ORIGIN OF THE TRANSIENT SPECTRUM

For the model (1) the origin of the anomaly can be traced to the question of existence of a solution of the similarity equation (16) which has the correct behaviour *both* for the wake and the tip. Written in terms of x rather than b and re-scaled to get rid of the constant, C, the similarity equation is

$$\frac{2}{x-3}\left(\eta\frac{dF}{d\eta}+xF\right)=\frac{d}{d\eta}\left(\eta^{\frac{11}{2}}\sqrt{F}\frac{d}{d\eta}\left(\eta^{-2}F\right)\right). \tag{20}$$

The parameters a and b which define the original similarity transformation, (15), expressed in terms of x are

$$a=-\frac{2x}{x-3}, \qquad b=\frac{2}{x-3}. \tag{21}$$

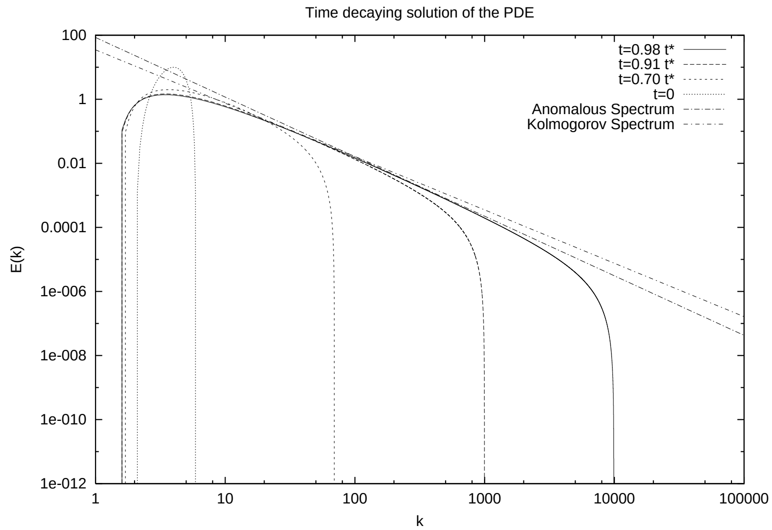

FIG. 6: Decaying time-dependent solutions beginning from compact initial data showing development of self-similar front with power law wake.

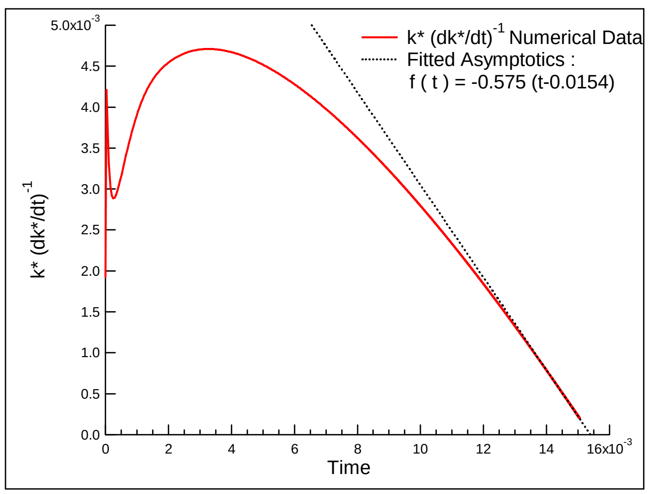

FIG. 7: Calculation of the asymptotic scaling properties of the self-similar solution for decaying case. The fitted line has slope $1/b = -0.575$ and t intercept $t^* = 0.0154$.

We require that equation (20) have a solution which behaves as η^{-x} as $\eta \to 0$ and also satisfies the boundary condition, (7), at the front tip, $\eta \to 1$. Such a solution is not typical and actually exists only for one value of x. In particular, such a solution does not exist for $x = 5/3$, the Kolmogorov value. The structure of the problem can be studied by introducing a new independent variable, $s = \log \eta$, and a pair of dependent variables, $f(s)$, $g(s)$ defined by

$$F = \frac{1}{25}\,\eta^{-3} f^2, \quad \frac{dF}{d\eta} = \frac{3}{25}\,\eta^{-4} f g. \tag{22}$$

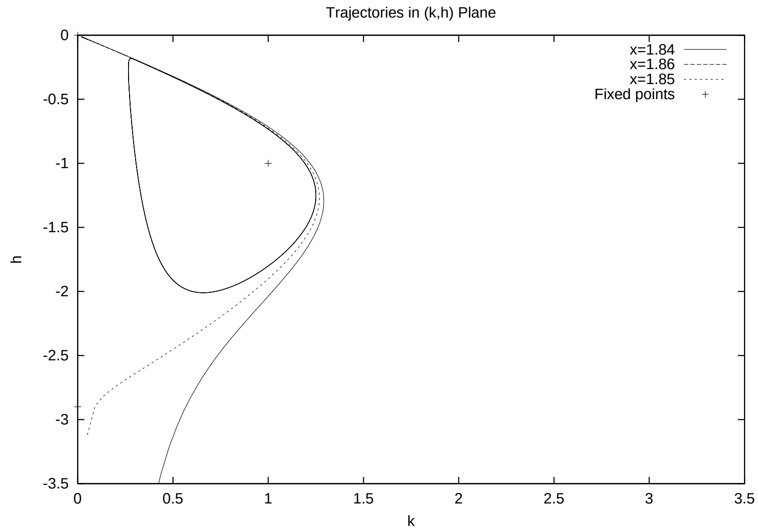

FIG. 8: Trajectories in the (k, h) plane.

The purpose of this transformation is to "autonomise" the equation[11]. That is, we remove the explicit dependence on η from the equation. When this is done, equation (20) is equivalent to the following autonomous first order system:

$$\begin{aligned} \frac{df}{ds} &= \frac{3}{2}(f+g) \\ f\frac{dg}{ds} &= \frac{1}{3}\left(5f^2 + 6fg - 9g^2 + \frac{10}{x-3}(3f+xg)\right), \end{aligned} \tag{23}$$

and methods of phase plane analysis can be applied. The associated dynamical system has three equilibria P1 $= (0, 0)$, P2 $= (0, 10/3(x-3))$ and P3 $= (1, -1)$. Note that P1 and P2 are singular points of the original equations, (23).

Let us now attempt to identify the trajectory in the (f, g) plane describing the physical solution. We note that the required trajectory must remain in the quadrant $f > 0$, $g < 0$. The wake is at $\eta \to 0$, or $s \to \infty$. In the wake, $F \sim \eta^{-x}$ and $F' \sim -x\eta^{-x-1}$. It follows that $f \sim \eta^{3-x}$ and $g \sim -x\eta^{3-x}$. The value of x is less than 3 so both f and g go to zero as $\eta \to 0$. The wake is therefore at $(0, 0)$ and should be reached as $s \to -\infty$.

Now consider the tip. We know that the front tip is at $\eta = 1$, or $s = 0$. Both F and F' go to zero as $\eta \to 1$ but it follows from (7) that the product $F^{-1/2}F'$ remains finite. The front tip therefore lies at some finite point on the negative g axis. In fact the tip lies at P2. To show this, we show that the moving boundary condition is satisfied there. Translating (7) into the self-similar variables we obtain

$$-b\tau^{b-1} = -\tau^{\frac{5}{2}b+\frac{1}{2}a} \lim_{\eta\to 1} \eta^{\frac{7}{2}} \frac{1}{\sqrt{F}} \frac{dF}{d\eta}. \tag{24}$$

Balancing the τ dependence gives us back the self-similarity condition, $a = -2 - 3b$. We now carefully do the various changes of variables and rescalings to obtain

$$b = \lim_{s\to 0} \frac{3}{5} g. \tag{25}$$

Noting the relations (21), we see that this condition is satisfied identically at the point P_2.

The critical value of x occurs when the unstable manifold of P_1 intersects the stable manifold of P_2 thus forming a connection between the two singular points of the original equations. This is then the only trajectory which can satisfy the required conditions to describe both the tip and the wake. A numerical approximation to the unstable manifold of the origin as x is varied through the critical value is shown in figure 8. The corresponding front profiles, converted back into the self-similar variables are shown in figure 9.

In practice, any model should include dissipation so that this self-similar solution above will be valid only until the front tip meets the dissipation scale. After this, the transient slope gets replaced in the inertial range by the stationary cascade solution, with or without bottleneck depending on the dissipation, as discussed above.

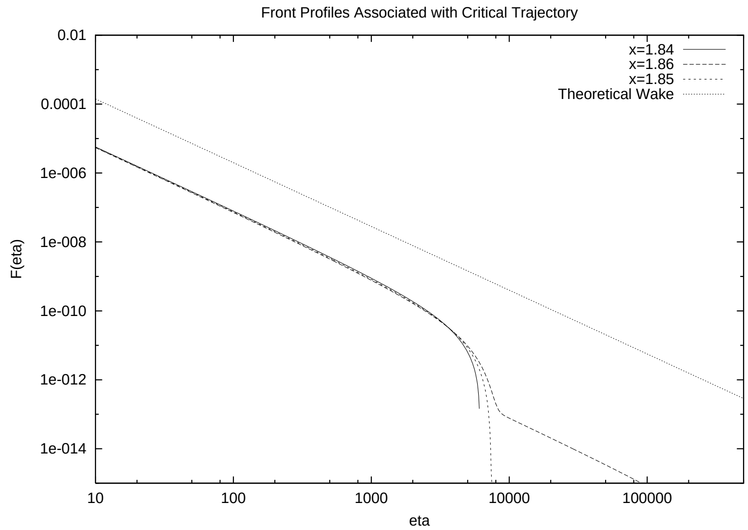

FIG. 9: Corresponding front profiles.

V. CONCLUSIONS

In summary, we presented a simple model in which basic properties of the Navier-Stokes turbulence are built-in: dimensionality and scaling, Kolmogorov and thermodynamic spectra. This model allows to obtain new predictions about the "warm" cascade states which are a nonlinear mixture of the cascade and thermodynamic solutions and which describe the bottleneck phenomenon. The model also allowed us to study the self-similar dynamics of the finite-time formation of the steady cascade states.

Acknowledgements

We thank Ildar Gabitov and Alan Newell for helpful discussions.

[1] K. Sreenivasan, Phys. Fluids **7**, 2778 (1995).
[2] R. Kraichnan and D. Montgomery, Reports on Progress in Phys. **43**, 547 (1980).
[3] G. Falkovich, Phys. **6**, 1411 (1994).
[4] A. Lacey, J. Ockendon, , and A. Tayler, SIAM J. Appl. Math. **42(6)**, 1252 (1982).
[5] C. Elliott and J. Ockendon, *Weak and Variational Methods for Moving Boundary Problems* (Pitman Advanced Publishing Program, Research Notes in Mathematics 59, Boston, 1982).
[6] B. Knerr, Trans. Am. Math. Soc. **234**, 381 (1977).
[7] S. Galtier, S. Nazarenko, and A. Newell, J. Plasma Physics **63(5)**, 447 (2000).
[8] C. Connaughton, A. Newell, and Y. Pomeau, to appear Physica D (2003).
[9] R. Kulsrud and S. Anderson, Astrophysical Journal **396**, 606 (1992).
[10] The parts 1 and 2 were inspired by the paper by Kulsrud and Anderson [9]. However, they used a 1st order in k equation which does not allow thermodynamic equilibria and which fails to describe spreading of the spectrum toward lower k.
[11] Simpler autonomising transformations can be certainly be found. The form of the transformation has been chosen in order to make more convenient the positions of the equilibrium points of the resulting dynamical system.